Optical transition probabilities and compositional dependence of Judd–Ofelt parameters of Nd^{3+} ions in fluoroindate glasses

A. Flórez [a,*], J.F. Martínez [a], M. Flórez [a], P. Porcher [b]

[a] *Laboratorio de Materiales Fotónicos, Departmento de Física, Universidad Industrial de Santander, UIS, A.A. 678, Bucaramanga, Colombia*

[b] *Laboratoire de Chimie Appliquée de l'Etat Solide, ENSCP, 11 rue Pierre et Marie Curie, F-75231, Paris cedex 05, France*

Abstract

Indium fluoride-based glasses constitute a new generation of materials for applications in the mid-infrared range. Fluoroindate glasses with the following compositions (in mol%): $(40 - x)InF_3$, $20ZnF_2$, $20SrF_2$, $16BaF_2$, $2GdF_3$, $2NaF$, and $xNdF_3$. with $x = 1.0, 1.5, \ldots, 4.0$ NdF_3 mol% were prepared in a dry box under argon atmosphere. The absorption spectra at room temperature in the spectral range 300–5000 nm were obtained. The experimental oscillator strengths, f_{exp}, were calculated from the areas under the absorption bands. Using Judd–Ofelt theory and the fit process of least square, the phenomenological intensity parameters Ω_λ ($\lambda = 2, 4, 6$) were obtained. From f–f intensity model the theoretical oscillator strengths f_{cal} are calculated. In order to evaluates potential applications of Nd^{3+} ions in fluoroindate glasses, the spectroscopy parameters: transition probability between multiplets $A_{JJ'}$, branching ratio $\beta_{JJ'}$, radiative lifetime τ_r, peak cross-section for stimulate emission ρ_p, for each band were obtained. The results were compared with those reported in the literature for similar glasses in the same concentrations and show that $^4F_{3/2} \rightarrow {}^4I_{11/2}$ transition has the most potential for laser application with a peak fluorescence at 1036 nm. © 2001 Elsevier Science B.V. All rights reserved.

1. Introduction

There is interest in the study of rare-earth-doped heavy metal fluoride glasses. These materials are transparent from ultraviolet (UV) to the infrared (IR) region; they can be easily prepared and a range of concentrations of transition metal and rare earth can be incorporated into the glass [1].

Besides the well-known zirconate glasses, several compositions based on indium fluoride, called fluoroindates, have been studied [2]. Compared to fluorozirconate glasses, these compositions have greater transparency in the mid-infrared range (up to 8 μm) smaller multiphonon emission rates, chemical stability, and are also more stable against atmospheric moisture [2–4]. We have recently described several optical properties of Er^{3+}, Pr^{3+} and Tm^{3+} ions in such glasses [5–11].

The Judd–Ofelt theory [12,13] is used to estimate the probability of forced electric dipole transitions. In this theory of f–f transitions, the so-called intensity parameters, Ω_λ, with $\lambda = 2, 4$ and 6, can be determined experimentally from the measurements of the absorption spectra and refractive index of the host material. From these parameters, several important optical properties,

* Corresponding author. Tel.: +57-97 644 7248; fax: +57-76 323 477.

E-mail address: aflorez@b-manga.cetcol.net.co (A. Flórez).

e.g., oscillator strengths, radiative transitions probabilities, branching ratios, spontaneous emission coefficients and peak cross-sections for stimulated emission [14], can be evaluated. In this paper, we have determined these quantities for the Nd^{3+} ion-doped fluoroindate glasses for several Nd^{3+} concentrations. A comparative analysis between fluoride and other glasses in similar concentrations is made.

2. Experimental

2.1. Glass preparation

The samples used in this study have the following composition (in mol%): $(40 - x)InF_3$, $20ZnF_2$, $20SrF_2$, $16BaF_2$, $2GdF_3$, $2NaF$, and $xNdF_3$. The InF_3 and NdF_3 were obtained using the ammonium bifluoride process [2]. An excess of NH_4FHF was added to the desired amount of oxides In_2O_3 and Nd_2O_3, in platinum crucible held at 400°C. To analyze the effect of the concentration on optical properties of Nd^{3+} in fluoroindate glasses the concentration, x, was varied from 1.0 to 4.0 (x: 1.0, 1.5, 2.0, 2.5, 3.0, 3.5, 4.0). All fluoride components were mixed and heated in a dry box under argon atmosphere at 700°C for melting and 850°C for fining. The liquid was then cast into a brass mold at 270°C and cooled to room temperature. Starting materials were chemical reagents (Aldrich and Merck, pro-analysis grade). The samples obtained were transparent and had pale lilac color. The samples were cut and polished into the shape of parallelepipeds.

2.2. Measurements

Density measurements were made using the Archimedean method in distilled water, and varied between 5.02 and 5.16 g/cm³, depending on the concentration of Nd^{3+} ion. The experimental error on the density was ±0.02. The refractive indices were measured using an Abbe refractometer, and the following indices were measured: 1.499 for the samples with x varying from 1.0 to 2.5; 1.510 for the sample with $x = 3.0$, and 1.525 for the samples with $x = 3.5$ and 4.0, with an accuracy ±0.005.

The absorption path lengths (l) of the samples were, respectively, 0.135 (1.0), 0.148 (1.5), 0.157 (2.0), 0.158 (2.5), 0.151 (3.0), 0.156 (3.5) and 0.131 cm (4.0) with an accuracy ±0.002.

Absorption spectra were measured at room temperature using a spectrophotometer (CARY 2400) in the spectral range from 300 to 2500 nm and a spectrophotometer (Perkin Elmer) from 2500 to 10,000 nm. The measured spectral absorptions were normalized using the sample thickness, l (cm), and the doping concentration, C (mol%). The thus modified spectra were used for the calculation of: oscillator strengths, phenomenological intensity parameters, Ω_λ, spontaneous emission transition probabilities, branching ratios, radiative lifetimes and peak cross-sections, using the intensity model as described previously [5–11].

3. Results

The absorption spectra of the Nd^{3+} occur due to the transition from the ground state $^4I_{9/2}$, to various excited states. The excited atoms relax via radiative or multiphonon transitions to the possible upper laser level in a shorter time compared to its radiative lifetime. Figs. 1 and 2 show the absorption spectrum of Nd^{3+} ion in fluoroindate glasses at room temperature for the sample of 3.5 mol% in the spectral range from 300 to 2500 nm
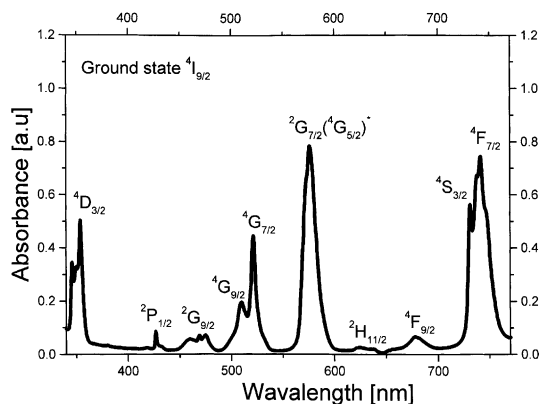

Fig. 1. Absorption spectrum of Nd^{3+} ion in fluoroindate glass at room temperature, in the spectral range from 340 to 760 nm. Sample with $x = 3.5$ mol% of Nd^{3+}.
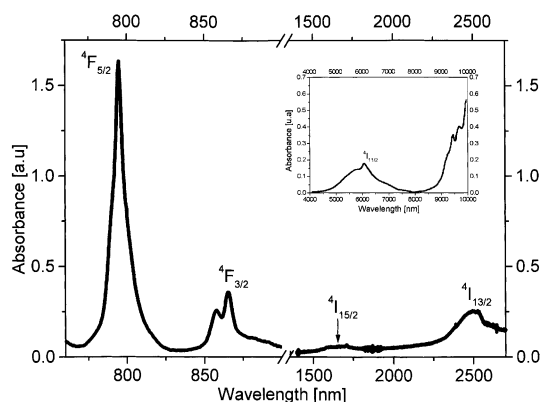
Fig. 2. Absorption spectrum of Nd^{3+} ion in fluoroindate glass at room temperature, in the spectral range from 760 to 2700 nm, and inset from 4000 to 10,000 nm. Sample with $x = 3.5$ mol% of Nd^{3+}.

and from 2500 to 10,000 nm. The spectrum for each sample has similar bands.

It is well established that OH^- content in glasses shifts the optical spectra from that observed for isolated Nd^{3+} ions [15]. The presence of a small amount of OH^- is confirmed from the shifts observed in the IR bands of the spectrum, Fig. 2.

Table 1 includes the transitions from $^4I_{9/2}$ identified in the studied spectral range, showing the transitions that are considered as having superimposed, the baricenter of each band or group of bands and the matrix elements of Carnall [14] are also included.

Table 2 includes the oscillator strengths obtained from the absorption spectra and calculated from the J–O model, the r.m.s. values, are also included. From these we observed that the better fit is obtained in the sample of 3.5 mol% (0.41×10^{-6}). The measured oscillator strengths show little variation and depend on the Nd^{3+} concentrations; only $^4F_{9/2}$ and $^2P_{3/2}$ transitions are almost independent of concentration. These values are in agreement with the reported N^{3+} ions in other glasses [16–19].

The intensity parameters, Ω_λ, determined from the least square fit of the measured absorption band intensities are given in Table 3. These parameters show the general tendency $\Omega_2 < \Omega_4 < \Omega_6$ in the seven samples studied. The same tendency is observed for Nd^{3+} ion in all glasses and crystals [20].

From the J–O parameters the spontaneous emission probability, $A_{JJ'}$, radiative lifetime, τ_r, the branching ratio, $\beta_{JJ'}$, and peak cross-section for stimulated emission, ρ_e, have been computed. The parameters obtained for any transitions are shown in Table 4.

The magnitude of ρ_e for the Nd^{3+}, $^4F_{3/2} \rightarrow {}^4I_{11/2}$ transition is directly related to the magnitude of the Ω_4 and Ω_6 parameters.

4. Discussion

The location, intensity and breadth of the absorption bands are determined by interaction of

Table 1
Energy values, J' states, oscillator strengths and matrix elements for Nd^{3+} in fluoroindate glasses (ground state $^4I_{9/2}$)[a]

Upper state from $^4I_{9/2}$	Energy (cm^{-1})	Matrix elements		
		$U_2{}^2$	$U_4{}^2$	$U_6{}^2$
$^4I_{11/2}$	1972	0.0194	0.1073	1.1652
$^4F_{3/2}$	11 533	0.0	0.2293	0.0549
$^4F_{5/2}{}^*$, $^2H_{9/2}$	12 537	0.0102	0.2451	0.5124
$^4F_{7/2}$, $^4S_{3/2}{}^*$	13 492	0.0010	0.0449	0.6597
$^4F_{9/2}$	14 715	0.0009	0.0092	0.0417
$^2H_{11/2}$	15 948	0.0001	0.0027	0.0104
$^4G_{5/2}{}^*$, $^2G_{7/2}$	17 328	0.9736	0.5941	0.0673
$^2K_{13/2}$, $^4G_{7/2}{}^*$, $^4G_{9/2}$	19 270	0.0664	0.2180	0.1271
$^2K_{15/2}$, $^2G_{9/2}{}^*$, $(^2D, ^2P)_{3/2}$, $^4G_{11/2}$	21 457	0.0010	0.0441	0.0364
$^2P_{1/2}{}^*$, $^2D_{5/2}$	23 440	0.0	0.0369	0.0021
$^4D_{3/2}$, $^4D_{5/2}{}^*$, $^2I_{11/2}$, $^4D_{1/2}$	28 526	0.0050	0.5257	0.0479

[a] Transition with greater contribution in the matrix elements. Systematic errors in the energy ± 50 cm^{-1}.

Table 2
Energy, experimental and calculated oscillator strengths (f_{exp}, f_{cal}) in unit of 10^{-6}, deviation and r.m.s. of Nd^{3+} in fluoroindate glasses for all concentrations $x = 1.0, 1.5, \ldots, 4.0$ in mol%[a]

E (cm^{-1})	1.0			1.5			2.0			2.5			3.0			3.5			4.0		
	f_{exp}	f_{cal}	Δ	f_{exp}	f_{cal}	Δ	f_{exp}	f_{cal}	Δ	f_{exp}	f_{cal}	Δ	f_{exp}	f_{cal}	Δ	f_{exp}	f_{cal}	Δ	f_{exp}	f_{cal}	Δ
1972	0.01	1.40	-1.39	0.69	1.47	-0.78	0.68	1.48	-0.80	1.02	1.48	-0.46	1.30	1.46	-0.16	1.16	1.46	-0.30	0.94	1.45	-0.51
11 533	1.34	1.28	0.06	1.45	1.35	0.10	1.57	1.47	0.10	1.50	1.38	0.12	1.52	1.40	0.12	1.47	1.33	0.14	1.20	1.33	-0.13
12 537	5.32	4.79	0.53	5.41	5.01	0.40	5.44	5.06	0.38	5.27	5.09	0.18	5.21	5.05	0.16	5.25	4.98	0.27	5.32	4.97	0.35
13 492	5.08	5.34	-0.26	5.20	5.58	-0.38	5.33	5.64	-0.31	5.34	5.64	-0.30	5.21	5.56	-0.35	5.21	5.56	-0.35	5.06	5.53	-0.47
14 715	0.35	0.40	-0.05	0.36	0.42	-0.06	0.35	0.42	-0.07	0.35	0.42	-0.07	0.36	0.42	-0.06	0.35	0.42	-0.07	0.36	0.42	-0.06
15 948	0.10	0.11	-0.01	0.08	0.11	-0.03	0.08	0.11	-0.03	0.08	0.12	-0.04	0.08	0.11	-0.03	0.08	0.11	-0.03	0.08	0.11	0.03
17 328	7.46	7.52	-0.06	7.59	7.67	-0.08	7.41	7.47	-0.06	7.49	7.57	-0.08	7.29	7.36	-0.07	7.29	7.36	-0.07	7.48	7.58	-0.10
19 270	4.09	3.12	0.97	4.46	3.25	1.21	4.24	3.26	0.98	4.48	3.30	1.18	4.40	3.29	1.11	4.11	3.20	0.91	4.73	3.22	1.51
21 457	1.28	0.78	0.50	1.20	0.82	0.38	1.22	0.83	0.39	1.19	0.83	0.36	1.24	0.83	0.41	1.19	0.81	0.38	1.18	0.81	0.37
23 440	0.23	0.33	-0.10	0.23	0.34	-0.11	0.25	0.35	-0.10	0.24	0.35	-0.11	0.24	0.36	-0.12	0.22	0.34	-0.12	0.24	0.34	-0.10
28 526	5.70	6.03	-0.33	5.97	6.34	-0.37	6.05	6.37	-0.32	6.21	6.52	-0.31	6.34	6.64	-0.30	5.96	6.24	-0.28	5.90	6.27	-0.37
r.m.s.	0.67×10^{-6}			0.58×10^{-6}			0.51×10^{-6}			0.50×10^{-6}			0.46×10^{-6}			0.41×10^{-6}			0.63×10^{-6}		

[a] Systematic error in the energy ±50 cm^{-1}.

Nd^{3+} ion with local crystalline fields. Each absorption band usually consists of a multiplicity of states. Unlike the local crystal field experienced by Nd^{3+} ion in crystalline hosts, the crystal field at sites in glasses varies from site to site. This distribution of crystal fields results in the inhomogeneous broadening of the absorption spectra of rare earth ions in amorphous media. Owing to this inhomogeneous broadening some bands are assumed to be superimposed because they are not resolved.

According to the J–O theory these oscillator strengths are a function of the three J–O parameters (Ω_2, Ω_4, Ω_6) and can be represented as linear combinations of these parameters. The J–O parameters are functions of crystal field parameters, intraconfigurational radial integral and energy separation of the 4f^N states and the opposite parity configurations. Hence, these parameters are dependent on the oscillator strengths and are found to vary from site to site. For Nd^{3+} ions the intensity of $^4I_{9/2} \rightarrow {}^4G_{5/2}$ transition is the principal determining factor for Ω_2. This transition satisfies the $|\Delta J|$, $|\Delta L| \leqslant 2$ and $\Delta S = 0$ selection rule for hypersensitive transitions [21]. This transition has the larger oscillator strength compared with all the other transitions. The Ω_2, involves the longer-range terms in the crystal field potential and is the most sensitive to local structure changes [21]. The variation of Ω_2 ($0.03 \leqslant \Delta\Omega_2 \leqslant 0.25$) indicates the homogeneity of the hosts, in this case, fluoroindate glasses. Also the relatively smaller Ω_2 ($<2.0 \times 10^{-20}$ cm^2) in all glasses studied indicates the covalence in the bonding [21].

From Table 1, since the matrix elements $\langle {}^4F_{3/2}\|U^2\|{}^4I_J \rangle$ are zero for the Nd^{3+} ion, Ω_2 will not have any affect on the stimulated emission parameters of Nd^{3+} ions [22]. The luminescence branching ratio can then be represented as dependent on only one parameter $Q = \Omega_4/\Omega_6$ which is usually considered as the spectroscopic quality factor [22]. Table 3 shows that in the samples studied, the Q is almost independent of the concentration. In practice, it has been observed that Q varies only in a narrow range.

Peak cross-sections are dependent on the intensity parameters, Ω_λ, and the bandwidth, $\Delta\lambda_{eff}$. Both are affected by composition changes. The

Table 3
Intensity parameters Ω_λ ($\lambda = 2, 4, 6$) for Nd^{3+} ion in fluoroindate glasses for all concentrations

Ω_λ ($\times 10^{20}$)	1.0	1.5	2.0	2.5	3.0	3.5	4.0
Ω_2	1.34	1.31	1.21	1.21	1.09	1.18	1.27
Ω_4	2.40	2.52	2.54	2.60	2.64	2.44	2.46
Ω_6	3.97	4.14	4.19	4.19	4.09	4.06	4.05
Ω_4/Ω_6	0.60	0.61	0.60	0.62	0.64	0.60	0.60
Error rms ($\times 10^{-20}$)	0.02	0.02	0.01	0.01	0.01	0.01	0.02

Table 4
Energy, radiative transition probabilities, branching ratios, radiative lifetimes and peak cross-sections (in units of 10^{-20} cm^2) of Nd^{3+} ion in fluoroindate glasses at room temperature[a]

Transition	Average energy (cm^{-1})	$A_{JJ'}$ (s^{-1})	ρ_e	$\beta_{JJ'}$	τ_r (ms)
$^4F_{3/2} \to {}^4I_{11/2}$	9561	384.77	1.87	0.3629	
$^4I_{9/2}$	11533	675.33	1.55	0.6370	0.9
$^4F_{5/2} \to {}^4I_{11/2}$	10565	1188.01	0.41	0.3743	
$^4I_{9/2}$	12537	1985.14	3.51	0.6254	0.3
$^4S_{3/2} \to {}^4I_{11/2}$	11520	2390.82	3.68	0.3828	
$^4I_{9/2}$	13492	3840.78	3.14	0.6150	0.16
$^4F_{9/2} \to {}^4I_{11/2}$	12743	89.50	0.12	0.3904	
$^4I_{9/2}$	14715	137.81	0.10	0.6062	4.36
$^4G_{5/2} \to {}^4F_{5/2}$	4791	125.97	10.48	0.0119	
$^4F_{3/2}$	5795	222.92	8.66	0.0211	
$^4I_{11/2}$	15356	4147.79	3.27	0.3933	
$^4I_{9/2}$	17328	5959.75	2.90	0.5652	0.09
$^4G_{7/2} \to {}^4F_{5/2}$	6733	97.69	1.35	0.0230	
$^4F_{3/2}$	7737	148.23	1.18	0.0350	
$^4I_{11/2}$	17298	1656.55	0.53	0.3910	
$^4I_{9/2}$	19270	2290.14	0.47	0.5405	0.23
$^2G_{9/2} \to {}^4I_{11/2}$	19485	426.63	0.06	0.3694	
$^4I_{9/2}$	21457	569.72	0.06	0.4933	0.86
$^4P_{1/2} \to {}^4S_{3/2}$	9948	109.15	2.11	0.0350	
$^4F_{5/2}$	10903	143.69	1.93	0.0460	
$^4D_{5/2} \to {}^2G_{9/2}$	7069	196.87	3.74	0.0057	
$^4G_{7/2}$	9256	441.95	2.86	0.0128	
$^4G_{5/2}$	11198	782.58	2.36	0.0228	
$^2H_{11/2}$	12578	1109.02	2.10	0.0323	

[a] Systematic error in the energy ± 50 cm^{-1}. Random error estimated to be $\leqslant 3\%$.

effective bandwidth is a measure of the overall extent of the Stark splitting of the J manifolds, and is inhomogeneous due to the site-to-site variations in the local fields with which the rare earth ion interacts. The intensity of the $^4F_{3/2} \to {}^4I_{11/2}$ laser transition is dependent only on the Ω_4 and Ω_6 parameters, because of the triangle rule $|J' - J| \leqslant \lambda \leqslant |J' + J|$ [23]. For a large cross-section, (assuming constant $\Delta\lambda_{eff}$) Ω_4 and Ω_6 should be as large as possible. In addition the fluorescence branching ratio to $^4I_{11/2}$ should be as favorable as possible. Since Ω_2 does not enter, the

branching ratios for Nd^{3+}, $^4F_{3/2}$ fluorescence can be expressed in terms of the ratio Ω_4/Ω_6.

In the Nd^{3+} ion, the only excited J manifold that is not relaxed predominantly by multiphonon process is the $^4F_{3/2}$ manifold [16]. This state fluoresces in four bands centered approximately at ≈ 880, ≈ 1060, ≈ 1350 and ≈ 1800 nm, corresponding transitions from the $^4I_{9/2}$, $^4I_{11/2}$, $^4I_{13/2}$ and $^4I_{15/2}$ excited states, respectively.

The observed fluorescence decays in neodymium glass are typically non-exponential even at the smallest concentration where ion–ion interactions

Table 5

Laser emission characteristics of some commercial Nd-doped phosphate glasses [20], for comparison with the sample of 3.5 mol% (FLU-35) analyzed in this work[a]

Glass	ED-2	ED-8	LG-650	LHG-5	P-107	EV-1	L-41	FLU-35
$\Delta\lambda_{eff}$ [nm]	30	36.1	33.5	25.5	26.5	21.7	32.5	14
λ_p [nm]	1062	1063	1059	1054	1054	1054	1056	1036
τ_{rad} [μs]	326	287	856	351	322	314	564	943
$\rho_e \times 10^{20}$ [cm^2]	2.9	3.1	1.1	3.9	3.9	4.7	1.9	1.87

[a] Random error estimated to be $\leqslant 3\%$.

are negligible. This non-exponential decay arises from the inhomogeneity of the samples. Different sites have different local fields and the odd harmonics in the expansion of these fields, which enter into the J–O parameters, have a site-to-site variation. The parameters determined from the integrated absorption spectra as in this case, are therefore an effective average over the different sites. The decay, on the other hand, is a summation of the decay of different sites having different decay rates. We find that the decay rate at early times may be less than the calculated radiative rate, while at later times in the decay it is greater. At larger neodymium concentrations, concentration quenching by ion–ion interaction becomes important. These interactions, however, also depend upon the line strength S_{ed} [16] and hence also reflect the effects of the compositional changes on the J–O parameters [24].

An examination of the energy levels, Table 1, and Figs. 1 and 2, shows that the $^2G_{9/2}$ J manifold has a larger energy than the $^4F_{3/2}$ J manifold by ≈ 9400 cm^{-1}. An electric-dipole transition between these manifolds could reduce the net cross-section for stimulated emission below that calculated for the $^4F_{3/2} \rightarrow {}^4I_{11/2}$ transition [16].

To compare the results of the emission parameters, $\Delta\lambda_{eff}$, λ_p, τ_{rad}, and ρ_e; in Table 5 we include the results obtained in this work, FLU-35, and those reported by Jacobs and co-workers [25] on some of the commercially available laser phosphate glasses. Although these glasses may have different compositions, the results are similar.

5. Conclusions

Our analysis shows that the J–O theory can be employed for predicting the relevant spectroscopic parameters associated with the possible laser transitions. As observed in all the other compositions, the three J–O parameters are ordered as $\Omega_2 < \Omega_4 < \Omega_6$. Comparison of the present results with other Nd^{3+}-doped glassy hosts shows agreement. From magnitudes of the radiative properties we suggest that $^4F_{3/2} \rightarrow {}^4I_{11/2}$ transition has the most potential for laser application with a peak fluorescence at 1036 nm. These data which show that rare-earth ions in fluoroindate glasses, are locally coordinated as in borate, phosphate and germanate glasses, making them potentially amenable to intensity analysis using the J–O model. The small Ω_2's in all samples may be associated with the micro-structural homogeneity around the Nd^{3+} ions. The fact of $\Omega_2 < 2.0$ indicates covalence in bonding.

Acknowledgements

References

[1] P.W. France (Ed.), Fluoride Glasses for Optical Fibers, Blackie, London, 1990.

[2] M. Poulain, G. Mazé, Chemtronics 3 (1998) 77.

[3] J.Y. Allain, M. Monerie, H. Pognant, Electron Lett. 26 (1990) 166.

[4] Y. Messaddeq, A. Delben, M.A. Aegerter, M. Poulain, J. Mater. Res. 8 (1993) 885.

[5] S.J.L. Ribeiro, R.E.O. Diniz, Y. Messaddeq, L.A.O. Nunes, M.A. Aegerter, Chem. Phys. Lett. 220 (1994) 214.

[6] A. Flórez, Y. Messaddeq, O.L. Malta, M.A. Aegerter, J. Alloys Compounds 227 (1995) 135.

[7] L.E.E. de Araujo, A.S.L. Gómes, C.B. de Araujo, Y. Messaddeq, A. Flórez, M.A. Aegerter, in: Nineth International Symposium on Non-Oxide Glasses (Halide Glasses), Hangzhou, China, 1994.

[8] L.E.E. de Araujo, A.S.L. Gomes, B.C.B. de Araujo, Y. Mesaddeq, A. Flórez, M.A. Aegerter, Phys. Rev. B 50 (22) (1994) 16219.

[9] G.S. Maciel, L. de Menezes, A.S.L. Gomes, C.B. de Araujo, Y. Messaddeq, A. Flórez, M.A. Aegerter, IEEE Photonics Technol. Lett. 7 (12) (1995) 1474.

[10] L.E.E. de Araujo, A.S.L. Gómes, C.B. de Araujo, Y. Messaddeq, A. Flórez, M.A. Aegerter, Appl. Phys. Lett. 68 (1995) 602.

[11] A. Flórez, M. Flórez, Y. Messaddeq, M.A. Aegerter, P. Porcher, J. Alloys Compounds 247 (1999) 215.

[12] B.R. Judd, Phys. Rev. 127 (1962) 750.

[13] G.S. Ofelt, J. Chem. Phys. 37 (1962) 511.

[14] W.T. Carnall, H. Crosswhite, H.M. Crosswhite, Energy Levels Structure and Transition Probabilities of the Trivalent Lanthanides in LaF_3, Argone National Laboratory, Report 1977.

[15] W.V. Moreshead, J.L.R. Nogues, R.H. Kravil, J. Non-Cryst. Solids 121 (1990) 267.

[16] W.F. Krupke, Phys. Rev. 145 (1966) 325.

[17] C. Brecher, L.A. Reisberg, Phys. Rev. B 18 (1978) 5799.

[18] Y. Subramanyan, L.R. Moorthy, S.V.J. Laksman, Phys. Chem. Solids 51 (1990) 1231.

[19] G. Amarnath, S. Buddhudu, J. Lumin. 47 (1991) 255.

[20] G. Ajith Kumar, P.R. Biju, C. Venugopal, N.V. Unnikrishnan, J. Non-Cryst. Solids 221 (1997) 47.

[21] R.D. Peacock, Struct. Bonding (Berling) 22 (1975) 83.

[22] A.A. Kaminski, in: Laser Crystals: Their Physics and Properties, Springer, Berlin, 1975.

[23] L.A. Resiberg, M.J. Weber, in: E. Wolf (Ed.), Progress in Optics, vol. XIV, Amsterdam.

[24] C. Layne, W. Lowdernilk, M. Weber, Relaxation Process in Laser Glass, Laser Program Annual Report, Rep. UCRL 5021-74, Lawrence Livermore Laboratory, Livermore, CA, 1974, p. 271.

[25] R.R. Jacobs, M.J. Weber, IEEE. J. Quant. Electron. 12 (1976) 102.